Modeling of nonlinear pulse propagation in periodic and quasi-periodic binary long-period fiber gratings

Gia-Wei Chern, Jui-Fen Chang, and Lon A. Wang

Institute of Electro-Optical Engineering, and Department of Electrical Engineering, National Taiwan University, Taipei, Taiwan

Received July 18, 2001; revised manuscript received January 10, 2002

A generalized transfer-matrix method is used to model nonlinear pulse propagation in a binary long-period fiber grating (LPFG). Two interface matrices are used to describe power coupling at the heterointerfaces, as in the linear case. Nonlinear phase shifts and pulse dispersion through the two basic regions are modeled by coupled nonlinear Schrödinger equations. Based on the generalized transfer-matrix model, a local intensity-dependent detuning parameter is introduced with which we investigate the general conditions for complete switching. Nonlinear switching in a quasi-periodic Fibonacci LPFG is also studied, and it is shown that complete switching can be achieved in such a quasi-periodic grating. © 2002 Optical Society of America

OCIS codes: 050.2770, 060.4370, 060.1810.

1. INTRODUCTION

Optical fibers are ideal for use in nonlinear interactions because they provide strong beam confinement over long propagation distances. Inasmuch as most optical fiber materials are subject to inversion symmetry, the nonlinear operation of devices made from such materials often utilizes the much weaker third-order Kerr-type nonlinearity.[1] A number of interesting phenomena have been observed and explored in both counterpropagating and copropagating waveguide configurations. Optical bistability[2,3] and Bragg grating solitons[4,5] are observed in nonlinear distributed-feedback structures. All-optical switching is shown in codirectional coupling devices such as nonlinear coherent directional couplers,[6–8] grating couplers,[9] and rocking filters.[10] Switching behaviors are also observed in other fiber-based devices including those with a Mach–Zehnder configuration[11,12] and nonlinear-optical loop mirrors.[13,14] The switching behaviors exhibit periodic variation with respect to input power because of their special interferometric configurations.

A long-period fiber grating (LPFG) was originally proposed for use as an all-fiber band-rejection filter.[15] The LPFG can couple light from the core mode to the copropagating cladding modes when the phase-matching condition is satisfied. Recently, optical switching, pulse reshaping, and optical limiting phenomena were observed in photoinduced LPFG's at pulse intensities in a range of several gigawatts per square centimeter.[16]

The nonlinear propagation of pulses with durations of a few tens of picoseconds has also been analyzed in detail by use of nonlinear coupled-mode equations.[17] Two types of typical intensity-dependent transmission were observed. For the first type, the central frequency of the pulse is adjusted to satisfy the linear phase-matching point. The energy transfer from core mode to cladding mode is almost complete when the input intensity is small. However, at high input intensity, the central intense portion of the pulse becomes detuned off resonance as a result of the Kerr effect and thus remains in core mode. Only the low-intensity wings of the pulse are coupled to the cladding mode. In this case the remainder of the high-intensity pulse in the core mode is narrowed. The second type, in which the central frequency of the pulse is near the transmission node of a linear LPFG, is the off-resonance case and is our main concern here. At low intensities the pulse remains almost entirely in the core mode. As the intensity is increased, the central high-power part of the pulse becomes detuned toward the phase-matching point and starts to couple to the cladding mode. The transmission curve exhibits a limiting characteristic at high input intensities. Such operation of the LPFG can thus serve as an optical limiting device. Based on these two basic operations, other schemes have also been proposed. For example, through cross-phase modulation a pump pulse can switch a weak signal pulse.[18] It was also shown that the intensity required for all-optical switching can be reduced to the order of 100 MW/cm^2 by the introduction of uniform phase-shifting regions within two LPFGs.[19]

In this paper first we extend our previously proposed transfer-matrix approach for the linear transmission properties of a photoinduced binary LPFG[20] to model nonlinear pulse propagation. The nonlinear transmission curve of an ideal binary LPFG is compared with that of a pure sinusoidal LPFG with the same grating strength. Based on this formalism and for a quasi-continuous-wave approximation, we introduce a local normalized detuning parameter. This detuning parameter is intensity dependent and plays a crucial role in the switching behavior of a LPFG. The effects of self-phase modulation and of cross-phase modulation on the nonlinear coupling of pulses in a LPFG can be analytically studied by use of

such a parameter. We consider mainly the off-resonance operation of a LPFG. Because nonlinear coupling is controlled by the instantaneous intensity, high- and low-intensity parts of the pulse will be directed into different output modes, and this will result in pulse breakup and degrade switching performance. The use of square pulses to prevent pulse breakup in nonlinear switching was proposed.[21] It is also found that the switching ratio in an LPFG can be greatly enhanced for a square pulse. To prevent the unnecessary complexities that would be introduced by the influence of pulse shape, we use a square pulse in the studies. For a given input intensity of the square pulse, we demonstrate that nonlinear transmission in a uniform LPFG can be equivalent to linear transmission in a chirped LPFG. This equivalence is based on the intensity-dependent local normalized detuning parameter and is a useful aid to understanding the switching behavior. General conditions of the detuning distribution for complete switching are also discussed. We apply the generalized transfer-matrix model to study the nonlinear transmissions of pulses over a quasi-periodic Fibonacci LPFG; almost complete switching is demonstrated when a square pulse is used as the input. Because a quasi-periodic grating lacks short-ranged order and the long-range order may be obscured by the introduction of nonlinearity, the method of determining the existence of complete switching is rather interesting. The evolution of power and local detuning is investigated and compared with that of a periodic LPFG. After local averaging, complete switching can be explained by the equivalency of a chirped linear grating.

The paper is organized as follows: In Section 2 a generalized transfer-matrix model for nonlinear pulse propagation in an ideal binary LPFG is developed. Also, parameters such as critical power and effective areas are introduced. In Section 3 we consider a quasi-cw pulse and introduce a local intensity-dependent detuning parameter that characterizes the in-phase superposition of couplings through the interfaces of adjacent periods. The nonlinear transmission of square pulses is also studied. Section 4 is devoted to analysis of nonlinear switching in a periodic LPFG. Through the analysis of the local detuning parameter, the transmission characteristics of a given intensity can be equivalent to those of a chirped LPFG in the linear coupling regime. We also discuss the general conditions of the slowly varying detuning parameter for the ideal complete switching. The nonlinear coupling characteristics of a quasi-periodic LPFG are discussed in Section 5. By using the nonlinear transfer-matrix model we demonstrate almost complete switching in a quasi-periodic LPFG which can be concisely explained by investigation of the local detuning parameters.

2. MODELING OF NONLINEAR PULSE PROPAGATION IN BINARY LONG-PERIOD FIBER GRATINGS

A model of the linear transmission properties of a binary LPFG was recently developed by Chern and Wang[20] and was based on the transfer-matrix method and mode perturbations. An ideal binary LPFG is composed of two basic regions, which we designate region 1 and region 0 in what follows. Region 0 is the usual fiber structure, whereas region 1 is exposed to UV irradiation and the core refractive index is thus increased by an amount Δn_{UV}. In the phase-matching condition, power couplings between core mode and cladding modes can occur in such a grating.[20,22] We use conventions introduced in Ref. 20 for quantities that belong to these two basic regions. Quantities written with overbars belong to region 0; the unbarred quantities are of region 1. For example, mode fields of the two regions are denoted $(\bar{\mathbf{e}}_j, \bar{\mathbf{h}}_j)$ and $(\mathbf{e}_j, \mathbf{h}_j)$, respectively, where the subscript j indicates the mode order, e.g., LP_{01} for the fundamental core mode and LP_{02} for the first cladding mode.[23] In our previous modeling of a binary LPFG we treated the mode fields of region 1 as perturbations of the unperturbed mode fields of region 0 and related the perturbation expansion coefficients to the conventional coupling constants. Here we shall assume that these mode fields satisfy the following orthogonal relations and are normalized to carry unity power:

$$\frac{1}{2}\int_{A_\infty} (\mathbf{e}_j \times \mathbf{h}_k) \cdot \hat{\mathbf{z}} \mathrm{d}A = \delta_{jk}, \tag{1}$$

where δ_{jk} is the Kronecker delta function. Similar expressions hold for the mode fields in region 0. As discussed in Ref. 22, in an LPFG we may consider only forward-propagating modes because the excited backward modes are small. The electric fields of an optical pulse in the two regions can be written as

$$\mathbf{E}(\mathbf{r}, t) = \sum_j A_j(z, t)\exp[i(\beta_j z - \omega_0 t)]\mathbf{e}_j, \tag{2a}$$

$$\bar{\mathbf{E}}(\mathbf{r}, t) = \sum_j \bar{A}_j(z, t)\exp[i(\bar{\beta}_j z - \omega_0 t)]\bar{\mathbf{e}}_j, \tag{2b}$$

where $A_j(z, t)$ and $\bar{A}_j(z, t)$ are the slowly varying envelopes of the pulse in mode j that belong to regions 1 and 0, respectively. β_j and $\bar{\beta}_j$ are the corresponding propagation constants, and ω_0 is the central frequency of pulse. When such a pulse crosses the heterointerface between the two regions, because of discontinuities in the guiding structures, mode couplings occur at such interfaces. We can derive the transmission coefficients by requiring continuity in the tangential electric and magnetic fields. Because this process is linear, the coupling between the mode amplitudes can be described by a matrix. For example, assume that a cw wave field with frequency ω is incident upon the heterointerface from region 0 to region 1; we may use the following matrix equation to describe the changes in mode amplitude:

$$\mathbf{A}(\omega) = \mathbf{F}^{(1|0)}(\omega)\bar{\mathbf{A}}(\omega). \tag{3}$$

Here we have used column vectors $\mathbf{A}(\omega) = [A_{01}^{\mathrm{co}}(\omega), A_{02}^{\mathrm{cl}}(\omega), A_{03}^{\mathrm{cl}}(\omega), \ldots]^{\mathrm{T}}$ to represent mode amplitudes of the cw wave field in region 1. Here, superscripts co and cl are used to denote core and cladding modes. The mode amplitudes in region 0 are treated similarly. And the interface matrix has the following form (the details of derivation can be found in Ref. 20):

$$\mathbf{F}^{(1|0)}(\omega) = \begin{bmatrix} 1 - D_{01}^{\mathrm{co}} & \dfrac{\kappa_{01-0\nu}^{\mathrm{co-cl}}}{\beta_{01}^{\mathrm{co}} - \beta_{0\nu}^{\mathrm{cl}}} \\ \dfrac{\kappa_{0\nu-01}^{\mathrm{cl-co}}}{\beta_{0\nu}^{\mathrm{cl}} - \beta_{01}^{\mathrm{co}}} & 1 - \dfrac{D_{0\nu}^{\mathrm{cl}}}{2} \end{bmatrix}, \tag{4}$$

where D_{01}^{co} and $D_{0\nu}^{\mathrm{cl}}$ are defined in Appendix A of Ref. 20 and they are included to satisfy power conservation to the second order in perturbation. $\kappa_{01-0\nu}^{\mathrm{co-cl}}$ is the conventional coupling constant in coupled-mode theory and is defined as[22]

$$\kappa_{01-0\nu}^{\mathrm{co-cl}}(\omega) = \frac{\omega\varepsilon_0 n_{\mathrm{co}}}{2}\Delta n_{\mathrm{UV}} \int_{A_{\mathrm{co}}} \mathbf{e}_{t01}^{\mathrm{co}*}(\omega)\mathbf{e}_{t\ 0\nu}^{\mathrm{cl}}(\omega)\mathrm{d}A. \tag{5}$$

Note that the coupling constant is a function of frequency ω. In addition, all the coefficients $D = D(\omega)$ and $\beta = \beta(\omega)$ in Eq. (4) are functions of frequency. Thus in the time domain we may use the following response matrix to describe the coupling of the pulse in the two modes:

$$\mathbf{A}(t)\exp(-i\omega_0 t) = \int_{-\infty}^{t} \mathbf{F}^{(1|0)}(t - t')\bar{\mathbf{A}}(t')\exp(-i\omega_0 t')\mathrm{d}t', \tag{6}$$

where $\mathbf{A}(t) = [A_{01}^{\mathrm{co}}(t), A_{02}^{\mathrm{cl}}(t), A_{03}^{\mathrm{cl}}(t), \ldots]^{\mathrm{T}}$ and $\mathbf{F}^{(1|0)}(t)$ is the Fourier transform of $\mathbf{F}^{(1|0)}(\omega)$. However, if the duration of the pulse is tens of picoseconds, as in the descriptions that follow, the spectra of the amplitudes $A(\omega)\exp(-i\omega_0 t)$ will be quite narrowly centered at ω_0. In such quasi-cw pulses we may use the following approximation for Eq. (6):

$$\mathbf{A}(t) \cong \mathbf{F}^{(1|0)}(\omega_0)\bar{\mathbf{A}}(t). \tag{7}$$

Similar expressions can be used for pulses that cross the interfaces from region 1 to region 0, and the corresponding interface matrix is

$$\mathbf{F}^{(0|1)}(\omega) = \begin{bmatrix} 1 - \dfrac{D_{01}^{\mathrm{co}}}{2} & \dfrac{-\kappa_{01-0\nu}^{\mathrm{co-cl}}}{\beta_{01}^{\mathrm{co}} - \beta_{0\nu}^{\mathrm{cl}}} \\ \dfrac{-\kappa_{0\nu-01}^{\mathrm{cl-co}}}{\beta_{0\nu}^{\mathrm{cl}} - \beta_{01}^{\mathrm{co}}} & 1 - \dfrac{D_{0\nu}^{\mathrm{cl}}}{2} \end{bmatrix}. \tag{8}$$

As for the propagation through the two regions, the evolution of mode amplitudes may be described by the following coupled equations (here we take region 1 for example)[17,19,24]

$$\frac{\partial A_{01}^{\mathrm{co}}}{\partial z} + \frac{i}{2}\beta_{01}''^{\mathrm{co}}\frac{\partial^2 A_{01}^{\mathrm{co}}}{\partial \tau^2} = i\left(\gamma_{01-01}^{\mathrm{co-co}}|A_{01}^{\mathrm{co}}|^2 + 2\sum_{\mu}\gamma_{01-0\mu}^{\mathrm{co-cl}}|A_{0\mu}^{\mathrm{cl}}|^2\right)A_{01}^{\mathrm{co}}, \tag{9}$$

$$\left(\frac{\partial}{\partial z} + \Delta V_{g,\nu}\frac{\partial}{\partial \tau}\right)A_{0\nu}^{\mathrm{cl}} + \frac{i}{2}\beta_{0\nu}''^{\mathrm{cl}}\frac{\partial^2 A_{0\nu}^{\mathrm{cl}}}{\partial \tau^2} = i\left(\gamma_{0\nu-0\nu}^{\mathrm{cl-cl}}|A_{0\nu}^{\mathrm{cl}}|^2 + 2\gamma_{0\nu-01}^{\mathrm{cl-co}}|A_{01}^{\mathrm{co}}|^2 + 2\sum_{\mu\neq\nu}\gamma_{0\nu-0\mu}^{\mathrm{cl-cl}}|A_{0\mu}^{\mathrm{cl}}|^2\right)A_{0\nu}^{\mathrm{cl}}, \tag{10}$$

where $\beta_j'' \equiv \mathrm{d}^2\beta_j/\mathrm{d}\omega^2$ is the second derivative of the propagation constant with respect to frequency for mode j. $\tau \equiv t - (\mathrm{d}\beta_{01}^{\mathrm{co}}/\mathrm{d}\omega)z$ is the retarded time for the core mode. $\Delta V_{g,\nu}$ is the group-velocity difference between core and cladding modes $LP_{0\nu}^{\mathrm{cl}}$. And the nonlinear phase-modulation coefficients are defined as

$$\gamma_{jk} = \frac{n_2\omega_0}{c}\frac{\int_{A_\infty}|\mathbf{e}_j|^2|\mathbf{e}_k|^2\mathrm{d}A}{\int_{A_\infty}|\mathbf{e}_j|^2\mathrm{d}A\int_{A_\infty}|\mathbf{e}_k|^2\mathrm{d}A}, \tag{11}$$

where n_2 is the nonlinear Kerr index. Note that to be consistent with first-order perturbation treatment of interface coupling coefficients there is no need to distinguish γ_{jk} between the two regions. The effective area of mode j is related to the nonlinear phase-modulation coefficient as

$$A_{\mathrm{eff},j} = \frac{n_2\omega_0}{c\,\gamma_{jj}}. \tag{12}$$

Equations (9) and (10) describe the propagation of the pulses within regions 0 and 1 by taking into account the effects of dispersion, self-phase modulation, and cross-phase modulation. Combined with interface matrices (4) and (8), these constitute the governing equations to describe the propagation of a nonlinear pulse in a binary LPFG. In Fig. 1 we compare the transmission curves for a binary and a uniform sinusoidal LPFG with equal length and linear coupling strength. [Physically, the index modulations are chosen as Δn_{UV} (binary) $= \pi/4\Delta n_{\mathrm{UV}}$ (sinusoidal).] The modeling of a sinusoidal LPFG is based on the combined equations of coupled-mode theory and the nonlinear phase-modulation terms on the right-hand sides of Eqs. (9) and (10) (cf. Refs. 17 and 19). The guiding structure has a step-index profile, and the calculated modal properties can be found in detail in Ref. 22. The fiber parameters are as follows: $a_{\mathrm{co}} = 2.625\ \mu\mathrm{m}$, $a_{\mathrm{cl}} = 70\ \mu\mathrm{m}$, $n_{\mathrm{co}} = 1.456$, and $n_{\mathrm{cl}} = 1.45$. The resonant cladding mode is chosen to be the LP_{04} mode. The linear coupling constant $\kappa_{01-0\nu}^{\mathrm{co-cl}}\Lambda$ used in calculation is normalized as $\pi/2N$, where N is the number of cells in a binary LPFG, so complete linear switching can be achieved at the resonant wavelength. The nonlinear phase-modulation coefficients are $\gamma_{\mathrm{co-co}} = n_2\omega_0/cA_{\mathrm{eff,co}}$, with $A_{\mathrm{eff,co}} = 48.2\ \mu\mathrm{m}^2$, $\gamma_{\mathrm{co-cl}} = 8.67 \times 10^{-3}n_2\omega_0/c$, and

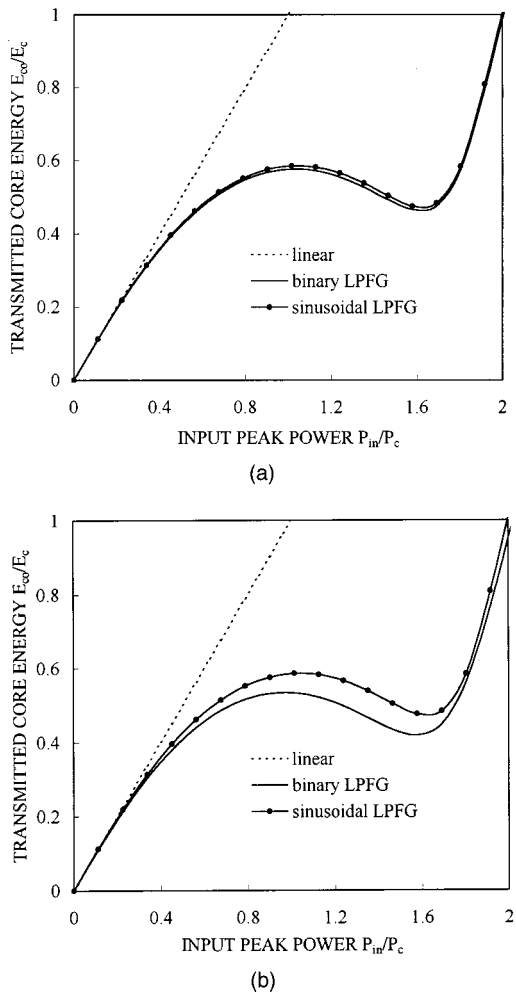

Fig. 1. Core energy transmitted through a binary and a uniform sinusoidal LPFG as a function of normalized input peak power. The number of unit cells is (a) 120 and (b) 15 in each grating. E_c is defined as the total energy of the pulse with input peak power P_c.

$\gamma_{\mathrm{cl-cl}} = 6.574 \times 10^{-3} n_2 \omega_0 / c$. The central wavelength of the pulse is $\lambda_0 = 1.55\ \mu$m and corresponds to off-resonant operation. The initial pulse is a transform-limited Gaussian pulse with half-width 60 ps. Besides, we normalize the input power by the critical power P_c that was introduced by Jensen for nonlinear coherent directional couplers of cw couplings[6] and is redefined in our case as

$$P_c = \frac{4\kappa_{01-0\nu}^{\mathrm{co-cl}}}{\gamma_{01-01}^{\mathrm{co-co}} - 2\gamma_{01-0\nu}^{\mathrm{co-cl}}}. \tag{13}$$

For Fig. 1(a) the number of cells is 120 ($L_g = 69.5$ mm). At this length the transmission curves of the two gratings are barely distinguishable in the linear limit and in higher-intensity regions where the pulse is detuned from the resonance. Little deviation is found at the power $\sim 1\ P_c$ at which nonlinear phase modulations bring the pulse into resonance. This deviation can be attributed to the difference in interplay between linear couplings and nonlinear phase modulations of the two gratings. For a sinusoidal LPFG, both processes are distributed along the grating, whereas, for a binary LPFG, couplings take place only at heterointerfaces between regions 0 and 1. However, when many fewer number of cells are compared, as for the case shown in Fig. 1(b), where $N = 15$ ($L_g = 8.7$ mm), a larger deviation at the critical power is observed, while two gratings remain similar in the linear limit and higher-intensity regions. This result implies that, as the number of periods decreases, the nonlinear coupling behaviors that are due to these two different mechanisms near the critical power are more distinct. However, at the intensity region where the pulse is detuned, these two gratings are almost the same.

3. QUASI-CONTINUOUS-WAVE APPROXIMATION AND INTENSITY-DEPENDENT DETUNING PARAMETERS

In this section we consider the quasi-cw approximation, which is mathematically equivalent to neglecting the dispersion terms in Eqs. (9) and (10). When the group-velocity difference is assumed small,[17] the solution to these two equations is that the mode amplitudes acquire an additional nonlinear phase shift as

$$\begin{aligned} A_{01}^{\mathrm{co}}(z,\ \tau) &= A_{01}^{\mathrm{co}}(0,\ \tau)\exp\{i\,\phi_{01}^{\mathrm{co}}[\mathbf{A}(0,\ \tau)]z\}, \\ A_{0\nu}^{\mathrm{cl}}(z,\ \tau) &= A_{0\nu}^{\mathrm{cl}}(0,\ \tau)\exp\{i\,\phi_{0\nu}^{\mathrm{cl}}[\mathbf{A}(0,\ \tau)]z\}, \end{aligned} \tag{14}$$

and the phase shifts per unit length are

$$\begin{aligned} \phi_{01}^{\mathrm{co}} &= \left[\gamma_{01-01}^{\mathrm{co-co}}|A_{01}^{\mathrm{co}}(0,\ \tau)|^2 + 2\sum_{\mu}\ \gamma_{01-0\mu}^{\mathrm{co-cl}}|A_{0\mu}^{\mathrm{cl}}(0,\ \tau)|^2\right], \\ \phi_{0\nu}^{\mathrm{cl}} &= \left[\gamma_{0\nu-0\nu}^{\mathrm{cl-cl}}|A_{0\nu}^{\mathrm{cl}}(0,\ \tau)|^2 + 2\gamma_{0\nu-01}^{\mathrm{cl-co}}|A_{01}^{\mathrm{co}}(0,\ \tau)|^2\right. \\ &\quad \left. + 2\sum_{\mu\neq\nu}\ \gamma_{0\nu-0\mu}^{\mathrm{cl-cl}}|A_{0\mu}^{\mathrm{cl}}(0,\ \tau)|^2\right]. \end{aligned} \tag{15}$$

Based on this result, the propagation of the quasi-cw pulse through region r can be described with the following matrix equation:

$$\mathbf{A}[\Lambda^{(r)},\tau] = \mathbf{P}^{(r)}[\mathbf{A}(0,\ \tau)]\mathbf{A}(0,\ \tau). \tag{16}$$

Here $z = 0$ is assumed to be the beginning of region r. When the phase shifts that are due to propagation constants are taken into account, the intensity-dependent phase-shift matrix is given by

$$\mathbf{P}^{(1)} = \begin{bmatrix} \exp\{i[\beta_{01}^{\mathrm{co}} + \phi_{01}^{\mathrm{co}}(\mathbf{A})]\Lambda^{(1)}\} & 0 \\ 0 & \exp\{i[\beta_{0\nu}^{\mathrm{cl}} + \phi_{0\nu}^{\mathrm{cl}}(\mathbf{A})]\Lambda^{(1)}\} \end{bmatrix}, \tag{17a}$$

and similarly for region 0:

$$\mathbf{P}^{(0)} = \begin{bmatrix} \exp\{i[\bar{\beta}_{01}^{\mathrm{co}} + \bar{\phi}_{01}^{\mathrm{co}}(\bar{\mathbf{A}})]\Lambda^{(0)}\} & 0 \\ 0 & \exp\{i[\bar{\beta}_{0\nu}^{\mathrm{cl}} + \bar{\phi}_{0\nu}^{\mathrm{cl}}(\bar{\mathbf{A}})]\Lambda^{(0)}\} \end{bmatrix}, \tag{17b}$$

where $\Lambda^{(1)}$ and $\Lambda^{(0)}$ are the lengths of regions 1 and 0, respectively. Let us denote by $\mathbf{A}_n(\tau)$ the mode amplitudes at the beginning of region 1 in the nth period of the grat-

ing. Then, by using interface transfer matrices (4) and (8), we can express the transmission of the quasi-cw pulse through a unit period by the following matrix equation:

$$\mathbf{A}_{n+1}(\tau) = \mathbf{F}^{(1|0)}(\omega_0)\mathbf{P}^{(0)}(\bar{\mathbf{A}}_n)\mathbf{F}^{(0|1)}(\omega_0)\mathbf{P}^{(1)}(\mathbf{A}_n)\mathbf{A}_n(\tau). \tag{18}$$

We now consider resonance between the core mode and a specific cladding mode $LP_{0\nu}$. The phase differences between rays coupled from core to cladding modes in the front and rear interfaces of regions 1 and 0 are just the differences in the arguments of the exponentials in Eq. (17):

$$\Delta^{(1)} \equiv (\beta_{01}^{\mathrm{co}} - \beta_{0\nu}^{\mathrm{cl}})\Lambda^{(1)} + [\phi_{01}^{\mathrm{co}}(\mathbf{A}) - \phi_{0\nu}^{\mathrm{cl}}(\mathbf{A})]\Lambda^{(1)}, \tag{19a}$$

$$\Delta^{(0)} \equiv (\bar{\beta}_{01}^{\mathrm{co}} - \bar{\beta}_{0\nu}^{\mathrm{cl}})\Lambda^{(0)} + [\bar{\phi}_{01}^{\mathrm{co}}(\bar{\mathbf{A}}) - \bar{\phi}_{0\nu}^{\mathrm{cl}}(\bar{\mathbf{A}})]\Lambda^{(0)}. \tag{19b}$$

From Eqs. (4) and (8), because the cross-coupling coefficients from region 0 to region 1 and from region 1 to region 0 differ by a factor of -1, in-phase coupling of the pulse through these two interfaces occurs when $\Delta^{(1)} = \pi$ and $\Delta^{(0)} = \pi$. We define the intensity-dependent phase-mismatch parameter of the nth period to be

$$\xi_n^{(1)}(\mathbf{A}_n) = \Delta_n^{(1)} - \pi, \tag{20a}$$

$$\xi_n^{(0)}(\bar{\mathbf{A}}_n) = \Delta_n^{(0)} - \pi. \tag{20b}$$

Assume that the duty ratio of each period is 0.5 and that in most cases the nonlinear phase-modulation coefficients satisfy $\gamma^{\mathrm{co-co}} \gg \gamma^{\mathrm{co-cl}}, \gamma^{\mathrm{cl-cl}}$; then the normalized detuning parameter within the nth period can be approximated as

$$\xi_n(\mathbf{A}_n) \cong \gamma_{01-01}^{\mathrm{co-co}}\Lambda_n|A_{01,n}^{\mathrm{co}}|^2 + \delta_n\Lambda_n, \tag{21}$$

where δ_n is the conventional definition of a linear detuning parameter with period Λ_n:

$$\delta_n = (\beta_{01}^{\mathrm{co}} - \beta_{0\nu}^{\mathrm{cl}}) - \frac{2\pi}{\Lambda_n}. \tag{22}$$

From Eq. (22) we can see that efficient couplings, say, in-phase couplings, of the pulse occur at time components such that $\xi \cong 0$, and it is clear how the nonlinear phase modulations modify the resonance conditions.

For a nonlinear pulse propagating in a uniform LPFG, because of the intensity-dependent nonlinear phase modulation the coupling behavior is different for low- and high-intensity parts of the pulse. This difference results in eventual pulse breakup and incomplete switching. Because nonlinear complete switching can be realized through a dual-core fiber coupler by use of a square pulse,[21] here we investigate the transmission of a square pulse through a uniform LPFG. Figure 2 depicts the relative transmission curve for an almost ideal square pulse (FWHM, 75 ps), where the relative transmission is defined as the ratio of the integrated output power to the initial power and the input peak power is normalized to P_c. The input pulse's profile is shown schematically in the inset. The resonance cladding mode is chosen to be LP_{04}, as used in the simulation of Fig. 1. The central wavelength of the pulse is set to 1.55 μm, which corresponds to off-resonance operation. Grating strength $\Delta n_{\mathrm{UV}} = 2.51 \times 10^{-4}$ and the length of the LPFG are chosen to produce complete linear coupling at $\lambda_{\mathrm{res}} = 1.541\ \mu$m. It can be seen that the best switching ratio

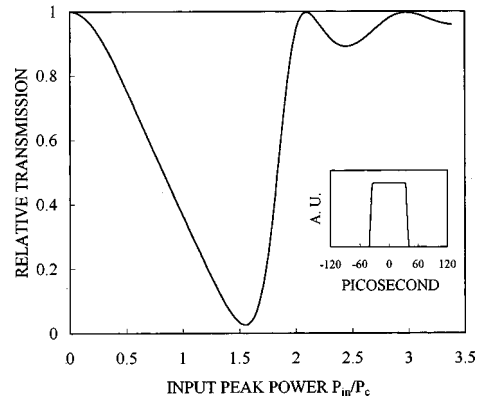

Fig. 2. Fraction of the output power emerging from the core plotted versus normalized input peak power for a 75-ps square pulse as input. Inset, normalized input pulse profile. This pulse profile is also used in Figs. 3, 4, and 6 below.

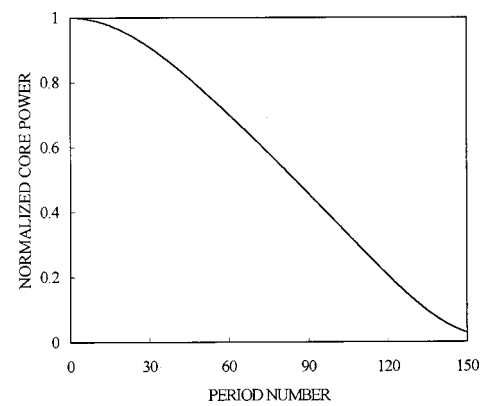

Fig. 3. Evolution of the normalized transmitted core power through a uniform LPFG with respect to input peak power $P_{\mathrm{in}} = 1.52\ P_c$ of the square pulse.

for the square pulse is more than 95% at the input peak power of $\sim 1.52\ P_c$. As was the case for Ref. 21, such an increased switching ratio for the square pulse is due to the breakup of the depressed pulse.

Figure 3 shows the evolution of normalized transmitted power along the LPFG with respect to the almost complete switching input peak power 1.52 P_c for the square pulse. In Section 4 we shall explore the complete coupling behavior by investigating the distribution of local detunings.

4. EQUIVALENCE OF NONLINEAR GRATING WITH CHIRPED LINEAR GRATING AND CONDITIONS FOR COMPLETE SWITCHING

From Eqs. (19) it can be seen that the phase differences between rays coupled from two adjacent interfaces of region 1 and 0 are intensity dependent. For a given intensity, the nonlinear phase modulation that contributes to the phase differences within a period can be regarded as an additional phase shift for linear coupling, i.e., the lengths of regions 1 and 0 are enlarged. Thus we can rewrite Eqs. (19) as

$$\Delta^{(1)} = (\beta_{01}^{\mathrm{co}} - \beta_{0\nu}^{\mathrm{cl}})\Lambda_{\mathrm{eff}}^{(1)}(\mathbf{A}), \tag{23a}$$

$$\Delta^{(0)} = (\bar{\beta}_{01}^{\mathrm{co}} - \bar{\beta}_{0\nu}^{\mathrm{cl}})\Lambda_{\mathrm{eff}}^{(0)}(\bar{\mathbf{A}}). \tag{23b}$$

Here we have defined the effective periods, $\Lambda_{\mathrm{eff}}^{(1)}$ and $\Lambda_{\mathrm{eff}}^{(0)}$, of the two basic regions. These effective periods depend on the intensity of the wave fields inside the corresponding regions; the explicit dependence can be found from Eqs. (19) and (23) as

$$\Lambda_{\mathrm{eff}}^{(1)}(\mathbf{A}) = \left[1 + \frac{\phi_{01}^{\mathrm{co}}(\mathbf{A}) - \phi_{0\nu}^{\mathrm{cl}}(\mathbf{A})}{\beta_{01}^{\mathrm{co}} - \beta_{0\nu}^{\mathrm{cl}}}\right]\Lambda^{(1)}, \tag{24a}$$

$$\Lambda_{\mathrm{eff}}^{(0)}(\bar{\mathbf{A}}) = \left[1 + \frac{\bar{\phi}_{01}^{\mathrm{co}}(\bar{\mathbf{A}}) - \bar{\phi}_{0\nu}^{\mathrm{cl}}(\bar{\mathbf{A}})}{\bar{\beta}_{01}^{\mathrm{co}} - \bar{\beta}_{0\nu}^{\mathrm{cl}}}\right]\Lambda^{(0)}. \tag{24b}$$

As the optical power is coupled between the core and the cladding along a uniform LPFG, an equivalent LPFG composed of chirped effective periods for linear coupling results. However, it is worth noting that the model of an equivalent chirped LPFG, which is designated for a specific intensity, favors square pulses rather than bell-shaped pulses to prevent the appearance of complexities introduced by the pulse shape. Such an equivalence is similar to the linear effective waveguide of spatial solitons proposed by Snyder *et al.*[25] Thus by using a square pulse of a certain intensity one can obtain the linear transmission spectrum of the equivalent chirped LPFG. With such a corresponding linear spectrum, we can explicitly show the intensity-dependent resonance shifts for nonlinear switching. To demonstrate this, we take the square pulse in Fig. 2 as an example. The central wavelength of the square pulse is 1.55 μm, which is that for off-resonance operation, and the parameters of the LPFG are the same as those discussed in Section 3. Figure 4(a) shows the spectra of the equivalent chirped LPFGs with input peak powers $P_{\mathrm{in}} = 10^{-4}$, 1.52, 2.25 P_c; and their corresponding effective periods derived from Eqs. (24) are shown in Fig. 4(b). It can be seen that when the input power is in the linear limit, as it is for $P_{\mathrm{in}} = 10^{-4}\,P_c$, the spectrum of the equivalent chirped LPFG is almost the same as the spectrum for linear transmission. This is so because the nonlinear phase-shift terms in Eqs. (24) can be neglected at such low intensity and thus the effective periods are almost unchanged. The pulse energy transferred from the core mode to the cladding mode is almost zero in this case. However, as the input peak power is increased, the spectrum of the equivalent chirped LPFG composed of effectively lengthened periods is shifted to longer wavelengths, and the transmission of the pulse starts to degrade from unity. Particularly at the power $P_{\mathrm{in}} = 1.52\,P_c$, the dip in transmission loss of the equivalent spectrum is just shifted to the central wavelength of the pulse, which is clearly consistent with the best switching contrast in Fig. 2. The decreasing effective periods along the LPFG shown in Fig. 4(b) manifest the process of continuing energy transfer from core mode to cladding mode. If the power is further increased, as can be seen for $P_{\mathrm{in}} = 2.25\,P_c$, even longer effective periods once again detune the transmission of the square pulse and result in worse switching behavior. This situation corresponds to the rising part of the relative transmission curve in the higher intensity region illustrated in Fig. 2.

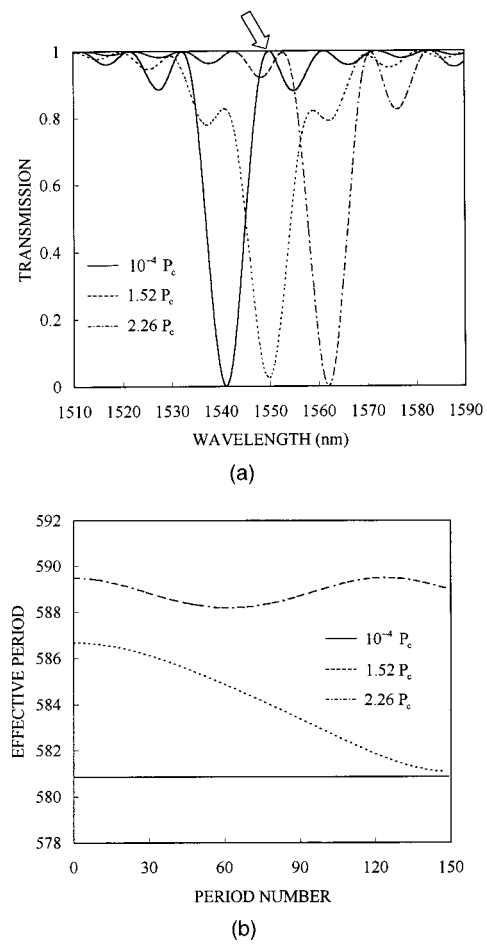

Fig. 4. (a) Transmission spectra of the equivalent chirped gratings for various input peak powers of the square pulse. The wavelength marked by the arrow is the center wavelength of the input pulse. (b) Effective periods of the equivalent chirped gratings for various input peak powers of the square pulse.

As we mentioned above, nonlinear coupling in a uniform LPFG for a square pulse of a chosen intensity can be regarded as linear coupling in an equivalent chirped LPFG. Additionally, we demonstrated in Section 3 that complete switching can be achieved for a square pulse with a specific intensity through a uniform LPFG. In contrast to complete linear switching in a uniform LPFG for which in-phase coupling, say, $\xi = 0$, is always satisfied,[22] nonlinear coupling implies that complete switching still occurs even if in-phase coupling is not maintained throughout the grating, whether for linear or nonlinear coupling. From the definition of the local detuning parameter in relation (21), the lengths of period and nonlinear phase modulation are the two factors that influence the variation of the detuning parameter along the grating. In what follows, we investigate the distribution of this parameter in several interesting cases, such as for complete linear switching in nonuniform binary LPFGs and for complete nonlinear switching in uniform LPFGs.

For simplicity, we first consider linear coupling in three typical nonuniform LPFGs whose spectra are depicted in Figs. 5(a), 5(c), and 5(e). These gratings correspond to a linear chirped grating, two uniform parts with different

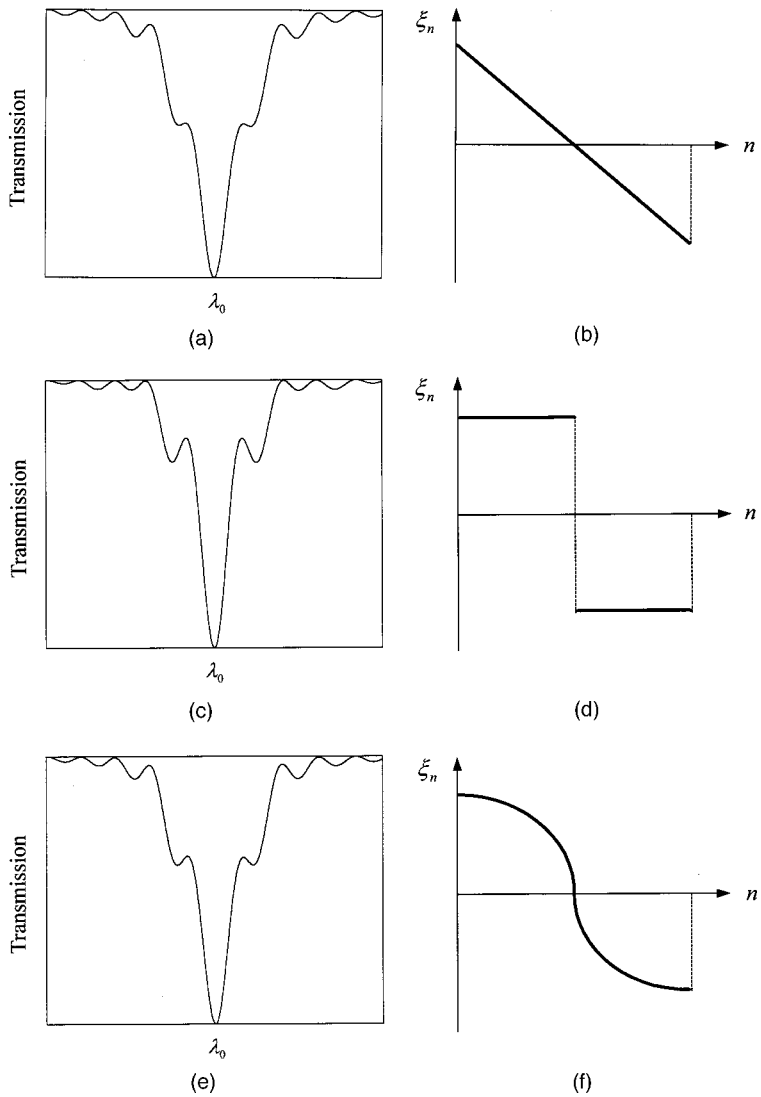

Fig. 5. (a), (c), (e) Transmission spectra of the three typical nonuniform LPFGs. Note that in each grating complete linear coupling occurs at wavelength λ_0. (b), (d), (f) Evolution of the normalized detuning parameters for wavelength λ_0 in the three nonuniform LPFGs that correspond to transmission spectra (a), (c), and (e), respectively.

grating periods, and a quadratic chirped grating, respectively. In each grating the existence of complete linear coupling at a certain wavelength λ_0 can be demonstrated by use of the generalized transfer-matrix method proposed in Section 2. Then, to show clearly the linear coupling process for wavelength λ_0 in three gratings, we plot the respective evolutions of normalized detuning parameter ξ in Figs. 5(b), 5(d), and 5(f). Assume that the total period numbers of LPFGs are the same as N; for these cases we find that there is a common feature: The distribution of ξ is halved and antisymmetrical with the grating center. Thus we have the following relation for the two halves (assume that $N = 2M$ in what follows):

$$\xi_{M-m} = -\xi_{M+m+1}, \qquad m = 0, 1, 2, \ldots, M - 1. \quad (25)$$

Here ξ_n is the normalized local detuning parameter of the nth period. Using this parameter, we can express the unit transfer matrix as follows[20]:

$$\mathbf{F}(\xi) \equiv \mathbf{F}^{(1|0)}\mathbf{P}^{(0)}\mathbf{F}^{(0|1)}\mathbf{P}^{(1)} = \begin{bmatrix} -\delta^2 \exp(-i\xi) + \gamma^2 & -\delta\gamma[1 + \exp(i\xi)] \\ \delta\gamma[1 + \exp(-i\xi)] & -\delta^2 \exp(i\xi) + \gamma^2 \end{bmatrix}. \quad (26)$$

The same notation as in Ref. 20 is used here and is not to be confused with the normalized detuning and nonlinear coupling coefficients. δ represents the self-coupling coefficient through the heterointerface, and we assume that this parameter is the same for core and cladding modes for ideal two-mode coupling.[20] γ is the cross-coupling coefficient of the core and cladding modes through the heterointerface. Inasmuch as the grating strength is kept constant, the unit transfer matrix of the nth period is exclusively a function of the corresponding local normalized detuning parameter; thus we have $\mathbf{F}_n = \mathbf{F}(\xi_n)$, where the dependence $\mathbf{F}(\xi)$ is given in Eq. (26). The total transfer matrices of the front and rear halves are

$$\mathbf{F}_{\text{front}} = \mathbf{F}(\xi_M)\mathbf{F}(\xi_{M-1})\ldots\mathbf{F}(\xi_2)\mathbf{F}(\xi_1), \tag{27}$$

$$\mathbf{F}_{\text{rear}} = \mathbf{F}(-\xi_1)\mathbf{F}(-\xi_2)\ldots\mathbf{F}(-\xi_{M-1})\mathbf{F}(-\xi_M). \tag{28}$$

Here we have utilized the antisymmetric distribution of the normalized detuning parameter [Eq. (25)]. In addition, from Eq. (26) it can be seen that, if ξ_n is replaced with $-\xi_n$, the unit transfer matrix satisfies the following relation:

$$\mathbf{F}(-\xi_n) = [\mathbf{F}(\xi_n)]^*. \tag{29}$$

Thus the transfer matrix of the rear half can be further written as

$$\mathbf{F}_{\text{rear}} = [\mathbf{F}(\xi_1)]^*[\mathbf{F}(\xi_2)]^*\ldots[\mathbf{F}(\xi_{M-1})]^*[\mathbf{F}(\xi_M)]^*. \tag{30}$$

However, because the unit transfer matrix in Eq. (26) is a unitary matrix, we may express the total transfer matrix of the front half, $\mathbf{F}_{\text{front}}$ in Eq. (27), as

$$\mathbf{F}_{\text{front}} = \begin{bmatrix} \alpha & \beta \\ -\beta^* & \alpha^* \end{bmatrix}. \tag{31}$$

Under the approximation of smooth coupling evolution that is applicable to general cases, it can be demonstrated that the $\mathbf{F}_{\text{rear}}$ in Eq. (30) has the following form (the explicit derivation can be found in Appendix A):

$$\mathbf{F}_{\text{rear}} = \begin{bmatrix} \alpha^* & \beta \\ -\beta^* & \alpha \end{bmatrix}. \tag{32}$$

Thus, combining Eqs. (32) and (33), we have the total N-period transfer matrix:

$$\mathbf{F}_{\text{tot}} = \mathbf{F}_{\text{rear}}\mathbf{F}_{\text{front}} = \begin{bmatrix} |\alpha|^2 - |\beta|^2 & 2\alpha^*\beta \\ -2\alpha\beta^* & |\alpha|^2 - |\beta|^2 \end{bmatrix}. \tag{33}$$

Assume that the input power is guided as a core mode and that the cladding mode is initially zero. From Eq. (33) note that, if $|\alpha| = |\beta|$, complete switching for the distribution of ξ in the form described by Eq. (25) can be achieved. Thus the magnitudes of the core mode and the cladding mode are the same at the half-length of the LPFG for complete switching.

Now we apply the above analysis to survey the complete switching of nonlinear coupling for a binary LPFG. Because the grating is uniform, the variation of detuning parameter ξ is due to the nonlinear phase shifts and is dependent on the evolution of the power in the core and the cladding modes. We plot in Fig. 6 the evolution of ξ along the grating. The input peak power is chosen for the best switching ratio of the square pulse shown in Fig. 2. The total number of periods for this LPFG is 150. One can find that the distribution of ξ approximately satisfies the general conditions outlined above, and this corresponds to the equivalent linear LPFG with negatively chirped periods [dashed curve in Fig. 4(b)]. In addition, as can be seen from Fig. 3, the evolution of the normalized transmitted power decreases smoothly and approaches 0.5 as the wave field passes through the midpoint of the LPFG. Thus the half-power-splitting condition described above is satisfied. However, also note that in Fig. 6 the antisymmetry relation is not exactly satisfied for the distribution of ξ, which explains why the switching is not complete as it is for the ideal case.

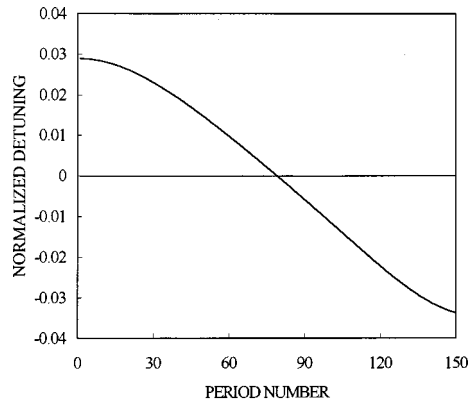

Fig. 6. Evolution of the normalized detuning parameters through a uniform LPFG with respect to input peak power $P_{\text{in}} = 1.52\,P_c$ of the square pulse.

5. NONLINEAR SWITCHING IN A QUASI-PERIODIC LONG-PERIOD GRATING

Recently, the transfer-matrix method based on perturbation expansion was used to study the transmission spectrum of a quasi-periodic LPFG.[20] In this section we further apply the generalized transfer-matrix method to modeling the nonlinear transmission in a Fibonacci LPFG. As demonstrated in Ref. 20, cladding mode resonances occur when the difference in the propagation constants matches the intrinsic Fourier peaks of the structure of the quasi-periodic grating. The resonance conditions are characterized by two independent integers that correspond to the underlying two incommensurate periods. We first show that the linear transmission properties of a quasi-periodic Fibonacci LPFG near a transmission dip is equivalent to a periodic LPFG of equal length with a prescribed grating period. This equivalence is important in the following analysis of the nonlinear coupling. By applying the nonlinear transfer matrix model developed in Sections 2 and 3 to a quasi-periodic Fibonacci grating, we demonstrate intensity-dependent switching. In addition, when a square pulse is used as input, almost complete switching can be found. From analysis of the evolution of optical power and the distribution of the local detuning parameters, the nonlinear switching can be qualitatively explained.

In general, a quasi-periodic grating is defined by the underlying of Bravais lattices. After the Bravais points are defined, each point is placed on a diffractor, which may be a simple region 1 with length $\Lambda^{(1)}$. One can derive the resonance condition by evaluating the structure of an infinite grating. The corresponding Bravais lattice and the structure of a quasi-periodic Fibonacci grating were introduced in Ref. 20. As has been demonstrated, the Fibonacci grating can also be constructed in a recursive way, and the equivalence is also confirmed.[26] We first define two basic blocks, designated block A and block B. A common definition for the fundamental blocks is as follows: Block A is composed of region 1 with length $\Lambda^{(1)}$ and region 0 with length $\Lambda_A - \Lambda^{(1)}$, and block B is composed of region 1 with length $\Lambda^{(1)}$ and region 0 with length $\Lambda_B - \Lambda^{(1)}$. The total lengths of the two blocks are thus Λ_A and Λ_B, respectively. The Fibonacci multilayer of order j is defined recursively as $S^{[j]} = S^{[j-1]}|S^{[j-2]}$ for

$j \geqslant 2$, with $S^{[0]} = A$ and $S^{[1]} = AB$. From this definition, it is clear that the total grating length satisfies the Fibonacci relation $L^{[j]} = L^{[j-1]} + L^{[j-2]}$. From the structure factor, the resonance condition is

$$\beta_{01}^{\mathrm{co}} - \beta_{0\nu}^{\mathrm{cl}} = \frac{m(\tau - 1)\tau' + n\tau'}{\tau\tau' + 1}\frac{2\pi}{\Lambda_B}, \tag{34}$$

where m and n are two independent integers, $\tau = (1 + \sqrt{5})/2$ is the golden mean, and $1 + 1/\tau' = \Lambda_A/\Lambda_B$ is the ratio of the two fundamental blocks. In Eq. (34) the contribution of the self-coupling term has been neglected for simplicity of the following discussion. That equation can be simplified to the following form when $\tau' = \tau$:

$$\beta_{01}^{\mathrm{co}} - \beta_{0\nu}^{\mathrm{cl}} - (m + n\tau)\frac{2\pi}{\bar{\Lambda}} = 0, \tag{35}$$

where $\bar{\Lambda} = (\tau^2 + 1)\Lambda_B = \tau\Lambda_A + \Lambda_B$ is the averaged grating period. The physical meaning of the resonance condition can be further explored by use of the previously introduced normalized detuning parameters. We define the following normalized detuning parameters that correspond to a specific resonance (m, n) for the two fundamental blocks as

$$\xi_A = \Delta_A - 2n\pi = (\beta_{01}^{\mathrm{co}} - \beta_{0\nu}^{\mathrm{cl}})\Lambda_A - 2n\pi, \tag{36a}$$

$$\xi_B = \Delta_B - 2m\pi = (\beta_{01}^{\mathrm{co}} - \beta_{0\nu}^{\mathrm{cl}})\Lambda_B - 2m\pi. \tag{36b}$$

Because for a Fibonacci sequence the number of blocks A is τ times that of block B,[26] we define the averaged detuning parameter $\bar{\xi}$ for a Fibonacci grating as

$$\bar{\xi} \equiv \frac{\tau}{1 + \tau}\xi_A + \frac{1}{1 + \tau}\xi_B. \tag{37}$$

Then phase-matching condition (34) can be rewritten as

$$\bar{\xi} = 0 \quad \text{or} \quad \tau\xi_A + \xi_B = 0. \tag{38}$$

The phase-matching condition corresponds to vanishing of the averaged normalized detuning parameter. The transmission spectrum of a Fibonacci LPFG is obtained by the transfer-matrix method as shown in Ref. 20. We have pointed out several features of this condition. First, a single cladding mode will contribute to several transmission-loss dips. Second, the transmission dips are grouped according to the resonance condition (m, n). In other words, a Fibonacci LPFG provides a mechanism that makes several cladding modes that belong to different groups overlap in a wavelength range. This phenomenon is quite different from the behavior of a uniform LPFG.

We now show that at an appropriate linear coupling strength a quasi-periodic Fibonacci LPFG near a resonance dip is actually equivalent to a periodic grating with equal length and a corresponding normalized detuning parameter. The equivalence is based on the identity of overall transfer matrices. Let us denote the transfer matrix of a periodic LPFG with normalized detuning parameter ξ_P and total length L $\mathbf{F}_P(\xi_P, L)$, and similarly that of a Fibonacci LPFG $\mathbf{F}_{\mathrm{Fb}}(\bar{\xi}, L)$. The demonstration is based on mathematical induction. We assume that the equivalence between these two matrices is valid for

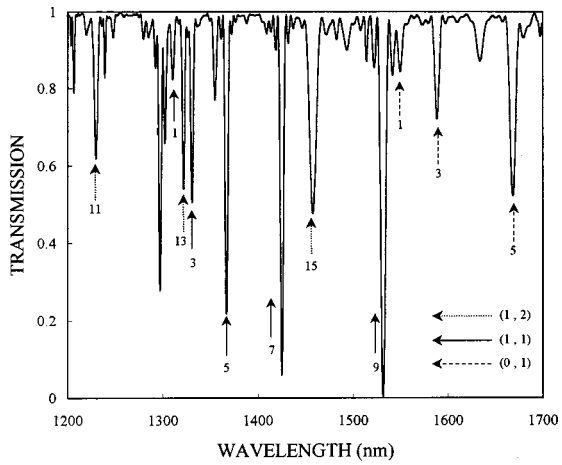

Fig. 7. Transmission spectrum of a quasi-periodic Fibonacci LPFG. The transmission dips are grouped according to resonance conditions (m, n). The first group corresponds to (1, 2), the second to (1, 1), and the third to (0, 1).

Fibonacci sequences of orders $j - 2$ and $j - 1$, i.e., $\mathbf{F}_{\mathrm{Fb}}^{[k]}(\bar{\xi}, L^{[k]}) \cong \mathbf{F}_P(\xi_P = \bar{\xi}, L^{[k]})$ for $k < j$. From the recursive construction of the Fibonacci multilayer, we have $\mathbf{F}_{\mathrm{Fb}}^{[j]} = \mathbf{F}_{\mathrm{Fb}}^{[j-1]}\mathbf{F}_{\mathrm{Fb}}^{[j-2]}$. By substituting the inductive assumption, we obtain $\mathbf{F}_{\mathrm{Fb}}^{[j]}(L^{[j]}) \cong \mathbf{F}_P(L^{[j-1]})\mathbf{F}_P(L^{[j-2]}) = \mathbf{F}_P(L^{[j-1]} + L^{[j-2]}) = \mathbf{F}_P(L^{[j]})$, where the recursive definition of the Fibonacci sequence is used. Thus the identity also holds for order j. And the inductive assumption is verified in our numerical calculations. In summary, we have the following equivalence:

$$\mathbf{F}_{\mathrm{Fb}}(\bar{\xi}, L) \cong \mathbf{F}_P(\xi_P = \bar{\xi}, L). \tag{39}$$

This equivalence accounts for the similarity of the transmission spectra near a resonance dip of a Fibonacci LPFG to a periodic spectrum and is important to the analysis of the switching behavior of the Fibonacci grating that we describe in what follows.

Next, to investigate the nonlinear switching in a Fibonacci LPFG we consider mainly the coupling of a pulse between the core mode and a specific cladding mode. Thus we prevent multicladding modes from overlapping near the wavelength of the pulse. Adjusting three basic parameters of a Fibonacci LPFG, namely, Λ_A, Λ_B, and $\Lambda^{(1)}$, results in the transmission spectrum of the grating that we designed for nonlinear application, as shown in Fig. 7. Grating strength Δn_{UV} is 3.3×10^{-4}, and parameter τ' is set to the golden mean. The average period of grating $\bar{\Lambda}$ is 1050 μm, and length $\Lambda^{(1)}$ is 200 μm. The number of periods is 144, which corresponds to the 10th Fibonacci sequence. As shown in Fig. 7, we label each dip with a different cladding mode number and use arrows of different styles to indicate the corresponding groups. Note that the $\nu = 9$ cladding mode that belongs to resonance condition (1, 1) is a good candidate for our nonlinear study because of its isolation and complete linear coupling. Even though optical power is also coupled from the core mode to several cladding modes that belong to different groups near this wavelength region, the nonlinear effect of these cladding modes can be neglected because the couplings are weak. Then we assume two-mode nonlinear coupling between the core mode and the

LP_{06} cladding mode, and linear coupling for those weak cladding modes. The central wavelength of the input square pulse is set to 1.539 μm for off-resonance operation, which corresponds to the maximum transmission in the long-wavelength side of the LP_{06} cladding mode. For a 50-ps square input pulse the relative transmission curve is as shown in Fig. 8. Except for a little degraded linear transmission that is due to coupling to several weak cladding modes at this wavelength, the figure shows the existence of intensity-dependent switching for the Fibonacci LPFG, just as for a uniform LPFG. And complete switching is almost achieved at the input peak power of $P_{\text{in}} = 1.15\,P_c$. To understand the local coupling behavior in the Fibonacci LPFG, we chose the input peak power $P_{\text{in}} = 1.15\,P_c$ as an example because it had the best switching ratio. Figure 9 shows the evolution of the normalized transmitted power. It can be found that, except for a little fluctuation along the length of the Fibonacci LPFG, the evolution curve is similar to that shown in Fig. 3. Accordingly, to investigate such a local coupling process we plot the evolution of the intensity-dependent detuning parameter in Fig. 10(a). It can be observed that the distribution of the detuning parameter separates into two curves that belong to variations of blocks A and B and that the parameter jumps between these two curves locally. However, the averaged normalized detuning parameter, which can be clearly seen in Fig. 10(b), lies on a smooth curve similar to the one discussed in Section 4 for complete switching, i.e., the antisymmetric distribution. Thus the almost complete nonlinear switching behavior can be understood from the equivalence between the Fibonacci and the periodic LPFG with an adiabatically varying normalized detuning parameter in expression (39).

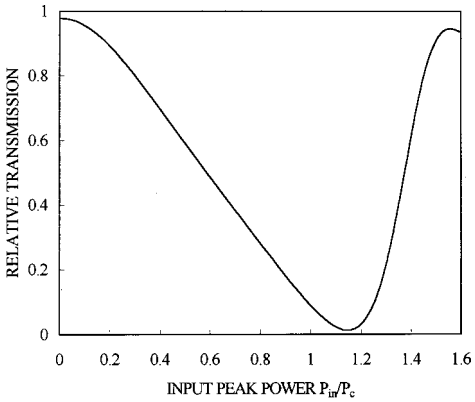

Fig. 8. Relative transmission of a square pulse in a Fibonacci LPFG as a function of normalized input peak power. Note that almost complete switching occurs at 1.15 P_c.

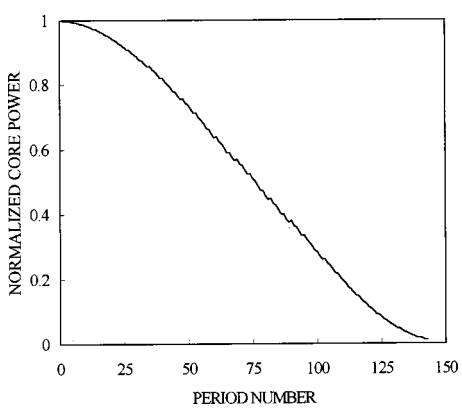

Fig. 9. Evolution of the normalized transmitted core power through a Fibonacci LPFG with respect to input peak power $P_{\text{in}} = 1.15\,P_c$ of a square pulse.

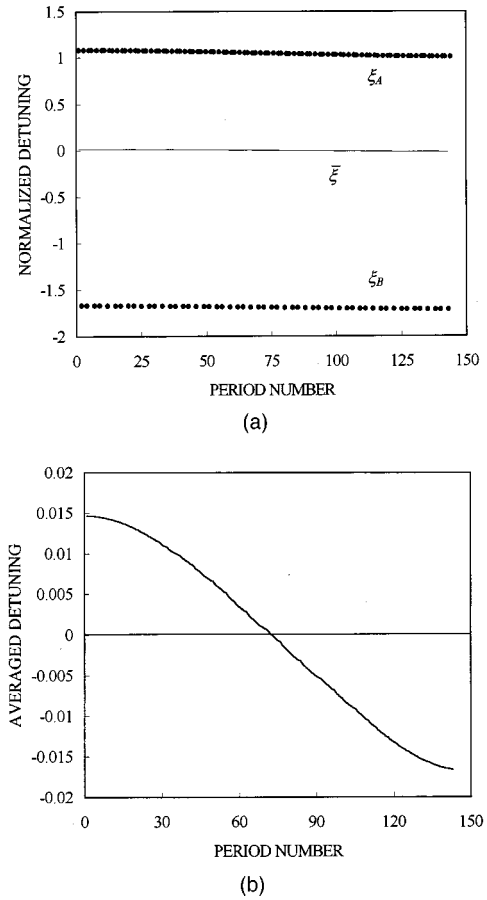

Fig. 10. (a) Filled circles, evolution of the normalized detuning parameters in a Fibonacci LPFG with respect to input peak power $P_{\text{in}} = 1.15\,P_c$ of a square pulse. Solid curve represents the corresponding evolution of the averaged normalized detuning parameters. (b) Illustration of the evolution of the averaged normalized detuning parameters.

6. CONCLUSIONS

The utilization of a transfer-matrix method to model nonlinear pulse propagation in a binary LPFG has been extended by inclusion of nonlinear phase modulations and dispersion. In contrast to those in a sinusoidal LPFG, power couplings in a binary LPFG take place only at the heterointerfaces between regions 0 and 1, and the effects of dispersion and nonlinear phase modulation occur only within regions 0 and 1. At the quasi-cw approximation the effect of dispersion can be neglected. Thus mode propagation through regions 0 and 1 can be found by use of intensity-dependent matrix equations. We then introduced an intensity-dependent normalized detuning parameter with which to evaluate the phase mismatch within a period. This parameter provides a physical in-

sight into the reason that the nonlinear phase modulation influences the local coupling. When a binary LPFG is compared to a uniform sinusoidal LPFG with equal length and linear coupling strength, the deviations between two gratings owing to nonlinear phase modulation are found at the intensity when the pulse is brought into resonance. Moreover, as a shorter grating length is chosen, these deviations are shown to become larger.

Because pulse breakup in LPFGs results in a limited switching ratio for a conventional bell-shaped pulse, we have demonstrated that the switching contrast is increased significantly by use of a square pulse as input. Complete switching can be achieved for an ideal square pulse if the input power is carefully controlled. By using a square pulse, we show the equivalence of the nonlinear coupling in a uniform LPFG and the linear coupling in a chirped LPFG. Thus the intensity-dependent spectrum composed of equivalent chirped periods can be obtained. It is also shown that an antisymmetric distribution of the normalized detuning parameters can result in complete switching. By analyzing the distribution of the normalized detuning parameter we can understand the coupling in a chirped linear grating and the switching in a nonlinear phase-modulated grating in a unified way. Finally, we utilized the generalized transfer-matrix method to study nonlinear switching in a Fibonacci LPFG. The phase-matching condition for a Fibonacci LPFG was formulated by use of the normalized detuning parameters, and the equivalence of the Fibonacci LPFG to a periodic grating with equal length and normalized detuning parameter has been demonstrated. The existence of nonlinear switching in a Fibonacci LPFG was demonstrated for the first time to our knowledge, and the local power evolution and distribution of a normalized detuning parameter were also studied to assist in our understanding of nonlinear switching behavior.

APPENDIX A. DISTRIBUTIONS OF DETUNING FOR COMPLETE SWITCHING

We prove a general condition of the detuning distribution for complete power switching. The variation of detuning parameter may be caused by period chirping or nonlinearity. As discussed in Section 4, if the distribution of the detuning parameter is antisymmetric with respect to the center of a binary grating, then complete switching can be achieved, provided that the power splitting ratio of the front half-grating is 0.5. In what follows, we demonstrate this property by using the transfer matrices. Let us express the transfer matrix of a unit period as

$$\mathbf{F} = \mathbf{P}^{(0)}\mathbf{F}^{(0|1)}\mathbf{P}^{(1)}\mathbf{F}^{(1|0)}. \tag{A1}$$

Then the transpose can be expressed as

$$\begin{aligned}\mathbf{F}^{\mathrm{T}} &= [\mathbf{F}^{(1|0)}]^{\mathrm{T}}\mathbf{P}^{(1)}[\mathbf{F}^{(0|1)}]^{\mathrm{T}}\mathbf{P}^{(0)} \\ &= \mathbf{F}^{(0|1)}\mathbf{P}^{(1)}\mathbf{F}^{(1|0)}\mathbf{P}^{(0)}.\end{aligned} \tag{A2}$$

From Eq. (30) for the transfer matrix of the rear half-grating we have

$$\begin{aligned}\mathbf{F}^{+}_{\mathrm{rear}} &= \mathbf{F}^{\mathrm{T}}_{M}\mathbf{F}^{\mathrm{T}}_{M-1}\ldots\mathbf{F}^{\mathrm{T}}_{1} = \prod_{k=M}^{1}\mathbf{F}^{\mathrm{T}}_{k} \\ &= \prod_{k=M}^{1}\mathbf{F}^{(0|1)}\mathbf{P}^{(1)}_{k}\mathbf{F}^{(1|0)}\mathbf{P}^{(0)}_{k} \\ &= [\mathbf{P}^{(0)}_{M}]^{-1}\left\{\prod_{k=M}^{1}\mathbf{P}^{(0)}_{k}\mathbf{F}^{(0|1)}\mathbf{P}^{(1)}_{k}\mathbf{F}^{(1|0)}\right\}\mathbf{P}^{(0)}_{1} \\ &= [\mathbf{P}^{(0)}_{M}]^{-1}\prod_{k=M}^{1}\mathbf{F}_{k}\mathbf{P}^{(0)}_{1} \\ &= [\mathbf{P}^{(0)}_{M}]^{-1}\mathbf{F}_{\mathrm{front}}\mathbf{P}^{(0)}_{1}.\end{aligned} \tag{A3}$$

Thus we have derived the relation of the transfer matrices between the front and the rear halves of a binary grating. As the grating is assumed to be lossless, transfer matrix $\mathbf{F}_{\mathrm{front}}$ may be written as

$$\mathbf{F}_{\mathrm{front}} = \begin{bmatrix}\alpha & \beta \\ -\beta^{*} & \alpha^{*}\end{bmatrix}. \tag{A4}$$

And, for wavelengths close to resonance, both phase matrices $\mathbf{P}^{(0)}_{M}$ and $\mathbf{P}^{(0)}_{1}$ may be approximated as diag(1, −1); then, from Eq. (A3), the transfer matrix of the rear half is

$$\mathbf{F}_{\mathrm{rear}} = \begin{bmatrix}\alpha^{*} & \beta \\ -\beta^{*} & \alpha\end{bmatrix}. \tag{A5}$$

L. A. Wang's e-mail address is lon@ccms.ntu.edu.tw.

REFERENCES AND NOTES

1. G. I. Stegeman and R. H. Stolen, "Waveguides and fibers for nonlinear optics," J. Opt. Soc. Am. B **6**, 652–662 (1989).
2. H. G. Winful, J. H. Marburger, and E. Garmire, "Theory of bistability in nonlinear distributed feedback structures," Appl. Phys. Lett. **28**, 379–381 (1979).
3. T. Hattori, N. Tsurumachi, and H. Nakatsuka, "Analysis of optical nonlinearity by defect states in one-dimensional photonic crystals," J. Opt. Soc. Am. B **14**, 348–355 (1997).
4. B. J. Eggleton, R. E. Slusher, C. M. de Sterke, P. A. Krug, and J. E. Sipe, "Bragg grating solitons," Phys. Rev. Lett. **76**, 1627–1730 (1996).
5. B. J. Eggleton, C. M. de Sterke, R. E. Slusher, and J. E. Sipe, "Distributed feedback pulse generator based on nonlinear fiber grating," Electron. Lett. **32**, 2341–2342 (1996).
6. S. M. Jensen, "The nonlinear coherent coupler," IEEE J. Quantum Electron. **18**, 1580–1583 (1982).
7. S. R. Friberg, A. M. Weiner, Y. Silberberg, B. G. Sfez, and P. S. Smith, "Femtosecond switching in a dual-core-fiber nonlinear coupler," Opt. Lett. **13**, 904–906 (1988).
8. S. Trillo, S. Wabnitz, E. M. Wright, and G. I. Stegeman, "Soliton switching in fiber nonlinear directional couplers," Opt. Lett. **13**, 672–674 (1988).
9. S. Trillo, S. Wabnitz, and G. I. Stegeman, "Nonlinear codirectional guided wave mode conversion in grating structures," J. Lightwave Technol. **6**, 971–976 (1988).
10. S. Trillo, S. Wabnitz, N. Finlayson, W. C. Banyai, C. T. Seaton, G. I. Stegeman, and R. H. Stolen, "Picosecond nonlinear polarization switching with a fiber filter," Appl. Phys. Lett. **53**, 837–839 (1988).
11. H. Kawaguchi, "Proposal for a new all-optical waveguide functional device," Opt. Lett. **10**, 411–413 (1985).
12. N. J. Doran and D. Wood, "Soliton processing element for all-optical switching and logic," J. Opt. Soc. Am. B **4**, 1843–1846 (1987).

13. N. J. Doran and D. Wood, "Nonlinear-optical loop mirror," Opt. Lett. **13**, 56–58 (1988).
14. J. D. Moores, K. Bergman, H. A. Haus, and E. P. Ippen, "Optical switching using fiber ring reflectors," J. Opt. Soc. Am. B **8**, 594–601 (1991).
15. A. M. Vengsarkar, P. J. Lemaire, J. B. Judkins, V. Bhatia, T. Erdogan, and J. E. Sipe, "Long-period fiber gratings as band rejection filters," J. Lightwave Technol. **14**, 58–65 (1996).
16. B. J. Eggleton, R. E. Slusher, J. B. Judkins, J. B. Stark, and A. M. Vengsarkar, "All-optical switching in long-period fiber gratings," Opt. Lett. **22**, 883–885 (1997).
17. J. N. Kutz, B. J. Eggleton, J. B. Stark, and R. E. Slusher, "Nonlinear pulse propagation in long-period fiber gratings: theory and experiment," IEEE J. Sel. Top. Quantum Electron. **3**, 1232–1245 (1997).
18. Y. Jeong and B. Lee, "Nonlinear property analysis of long-period fiber gratings using discretized coupled-mode theory," IEEE J. Quantum Electron. **35**, 1284–1292 (1999).
19. V. E. Perlin and H. G. Winful, "Nonlinear pulse switching using long-period fiber gratings," J. Lightwave Technol. **18**, 329–333 (2000).
20. G. W. Chern and L. A. Wang, "Transfer-matrix method based on perturbation expansion for periodic and quasi-periodic binary long-period gratings," J. Opt. Soc. Am. A **16**, 2675–2689 (1999).
21. A. M. Weiner, Y. Silberberg, H. Fouckhardt, D. E. Leaird, M. A. Saifi, M. J. Andrejco, and P. W. Smith, "Use of femtosecond square pulses to avoid pulse breakup in all-optical switching," J. Lightwave Technol. **25**, 2648–2655 (1989).
22. T. Erdogan, "Cladding-mode resonances in short- and long-period fiber grating filters," J. Opt. Soc. Am. A **14**, 1760–1773 (1997).
23. Recently a unified designation of modes was adopted for conventional single-core-mode fibers in which cladding modes are designated LP_{0n}, with $n = 2,3,\ldots$, whereas LP_{01} is related to a fundamental core mode. Another convention of cladding mode designation is the one used by Erdogan.[22] We shall use the former convention in this paper.
24. G. P. Agrawal, *Nonlinear Fiber Optics* (Academic, Boston, Mass., 1996).
25. A. W. Snyder, D. J. Mitchell, and L. Poladian, "Linear approach for approximating spatial solitons and nonlinear guided modes," J. Opt. Soc. Am. B **8**, 1618–1620 (1991).
26. D. Levine and P. J. Steinhardt, "Quasicrystals. I. Definitions and structures," Phys. Rev. B **34**, 596–616 (1986).